Acta Crystallographica Section F
Structural Biology and Crystallization Communications
ISSN 1744-3091

Structure of a 14-3-3σ–YAP phosphopeptide complex at 1.15 Å resolution

Benjamin Schumacher, Malgorzata Skwarczynska, Rolf Rose and Christian Ottmann*

Max Planck Institute of Molecular Physiology, Chemical Genomics Centre, Otto-Hahn-Strasse 11, 44227 Dortmund, Germany

Correspondence e-mail: christian.ottmann@cgc.mpg.de

Received 14 April 2010
Accepted 29 June 2010

PDB Reference: 14-3-3σ–YAP phosphopeptide complex, 3mhr.

The 14-3-3 proteins are a class of eukaryotic acidic adapter proteins, with seven isoforms in humans. 14-3-3 proteins mediate their biological function by binding to target proteins and influencing their activity. They are involved in pivotal pathways in the cell such as signal transduction, gene expression, enzyme activation, cell division and apoptosis. The Yes-associated protein (YAP) is a WW-domain protein that exists in two transcript variants of 48 and 54 kDa in humans. By transducing signals from the cytoplasm to the nucleus, YAP is important for transcriptional regulation. In both variants, interaction with 14-3-3 proteins after phosphorylation of Ser127 is important for nucleocytoplasmic trafficking, *via* which the localization of YAP is controlled. In this study, 14-3-3σ has been cloned, purified and crystallized in complex with a phosphopeptide from the YAP 14-3-3-binding domain, which led to a crystal that diffracted to 1.15 Å resolution. The crystals belonged to space group $C222_1$, with unit-cell parameters a = 82.3, b = 112.1, c = 62.9 Å.

1. Introduction

The 14-3-3 proteins are a class of eukaryotic acidic adapter proteins with seven isoforms in humans named with the Greek letters β, γ, ε, η, τ, σ and ζ and with a monomer molecular weight of around 30 kDa (Mhawech, 2005). Expression of 14-3-3 proteins can be found in practically all tissues (Hermeking, 2003; Hermeking & Benzinger, 2006). They are involved in the regulation of several hundred proteins, some of which play important roles in human diseases and in the life of the cell. Some examples are Raf kinases, p53, Cdc25, Cdk2 and HDACs (Hermeking, 2003; Tzivion *et al.*, 2006). 14-3-3 proteins mediate their biological function by binding to a target protein and thereby influencing its activity or localization. 14-3-3 proteins are involved in signal transduction, gene expression, enzyme activation, cell division and apoptosis. To date, more than 300 interacting proteins have been identified and include examples from most cellular processes (Hermeking & Benzinger, 2006).

14-3-3 proteins exist in the cell as dimers. It is known that 14-3-3 proteins can form homodimers and heterodimers (Ferl *et al.*, 2002). Each dimer has the possibility of binding two target proteins in the binding groove. The target protein is bound *via* a phosphorylated serine or threonine residue. The binding motifs have been identified and defined as mode I (RS*X*-pS/T-*X*P, where p indicates phosphate and *X* is any residue) and mode II (R*X*Φ*X*-pS/T-*X*P, where Φ is an aromatic or aliphatic residue) (Yaffe *et al.*, 1997; Muslin *et al.*, 1996). Recently, a third binding motif was added to the list which sits at the C-terminus of the target protein and shows the consensus sequence pS/pT-X_{1-2}-COOH (Ottmann, Marco *et al.*, 2007). In addition to phosphorylation-mediated interactions, 14-3-3 proteins can also bind to unphosphorylated partners (Ottmann, Yasmin *et al.*, 2007).

Although various crystal structures of 14-3-3 proteins in complex with peptides from target proteins have been solved, the crystallization of a full-length binding partner or of a fragment exceeding ten amino acids is a major problem. This is reflected in the structures deposited in the PDB with different target proteins of different

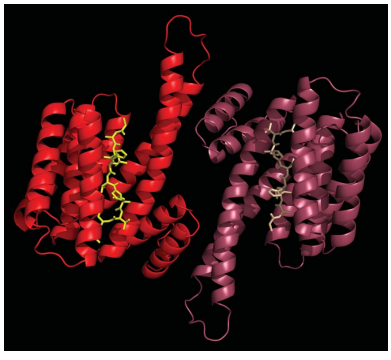

lengths. Several structures represent the binding of short (4–10 residues) phosphopeptides (PDB code 1qja, Rittinger *et al.*, 1999; PDB code 2c1n, Macdonald *et al.*, 2005; PDB code 3lw1, Schumacher *et al.*, 2010). A slightly longer 14-residue unphosphorylated binding peptide (PDB code 2o02; Ottmann, Marco *et al.*, 2007) shows the highest resolution to date of 1.5 Å for a 14-3-3 complex and represents an unphosphorylated binding mode. A tandem binding site of 31 amino acids (PDB code 2wh0; Kostelecky *et al.*, 2009) and a 52-residue dimeric interaction domain (PDB code 2o98; Ottmann, Yasmin *et al.*, 2007) represent the longest fragments. Finally, there is a nearly full-length partner consisting of 200 residues (PDB code 1ib1; Obsil *et al.*, 2001).

The Yes-associated protein (YAP) is a WW-domain protein and belongs to a functional family of proteins that also includes TAZ (transcriptional coactivator with PDZ-binding motif; Wang *et al.*, 2009) proteins. In humans, two transcript variants of 48 and 54 kDa exist. The binding motif for 14-3-3 proteins is the same in both isoforms and surrounds Ser127. By transducing signals from the cytoplasm to the nucleus, YAP is important for transcriptional regulation. The localization of YAP is controlled by phosphorylation. Various kinases from Hippo-like pathways and the mammalian LATS (large tumour suppressor) have been shown to be directly involved in the subcellular localization, transcriptional coactivator activities and biological functions of YAP and TAZ (Zhao *et al.*, 2007; Hao *et al.*, 2008; Lei *et al.*, 2008; Oka *et al.*, 2008; Zhang *et al.*, 2008). The interaction with 14-3-3 proteins after phosphorylation of Ser127 is important for nucleocytoplasmic trafficking.

Here, we report the cloning, expression, purification and crystallization of 14-3-3σ in complex with a YAP phosphopeptide, which led to crystals that showed diffraction to 1.15 Å resolution. The peptide represents the 14-3-3-binding site of the Yes-associated protein YAP and surrounds the phosphorylated residue pSer127 which is important for interaction.

2. Experimental methods

2.1. PCR and cloning of 14-3-3σ

The primers for the 14-3-3σ (NCBI GenBank BC000995.2) construct were obtained from Eurofins MWG Operon, Ebersberg, Germany. The primers were designed for cloning into pPROEX HTb expression vector (Invitrogen, Karlsruhe, Germany) with restriction sites for *Bam*HI and *Not*I endonucleases in the forward and reverse primers, respectively. The sequence of the forward primer was 5′-ATGGAGAGAGCCAGTCTGATC-3′ and that of the reverse primer was 5′-CGTCCACAGTGTCAGGTTGT-3′. The 14-3-3σ gene was amplified using 100 ng cDNA template (Open Biosystems, Huntsville, Alabama, USA). For the PCR, illustra Hot Start Master Mix (GE Healthcare, Freiburg, Germany) was used. The amount of each primer and the program were chosen as recommended by the manufacturer. The PCR product and the vector DNA were digested with *Bam*HI and *Not*I (NEB, Frankfurt am Main, Germany) simultaneously as recommended by the manufacturer. The DNAs were purified using the QIAquick PCR Purification Kit (Qiagen, Hilden, Germany) and ligated using the Quick Ligation Kit (NEB, Frankfurt am Main, Germany). The ligated construct was transformed into *Escherichia coli* XL10-Gold Ultracompetent cells (Stratagene, La Jolla, USA) according to the manual and positive clones were confirmed by sequencing. For expression, the positive construct was transformed into *E. coli* Rosetta (DE3) (Merck, Nottingham, England) according the manufacturer's recommendations.

2.2. Expression

E. coli Rosetta (DE3) cells (Merck, Nottingham, England) transformed with the cloned vector were used to inoculate 50 ml Luria–Bertani (LB) medium containing 100 µg ml^{-1} ampicillin. The culture was grown for 12 h at 310 K with vigorous shaking. The preculture was used to inoculate a 5 l Terrific Broth (TB) culture containing 100 µg ml^{-1} ampicillin. The culture was shaken at 140 rev min^{-1} at 310 K until an OD_{600} of 0.4–0.6 was reached. Protein expression was started by adding 0.4 m*M* IPTG to the culture. The culture was incubated at 298 K for 12 h and then harvested by centrifugation.

2.3. Protein purification

The bacterial pellet was resuspended in 50 ml lysis buffer containing 50 m*M* Tris–HCl, 300 m*M* NaCl, 5% glycerol, 10 m*M* imidazole, 0.5 m*M* TCEP and 1 m*M* PMSF pH 8.0. The cells were lysed using a microfluidizer (Microfluidics, Newton, Massachusetts, USA). The lysate was cleared by centrifugation at 95 000*g* for 30 min at 277 K. The His-tagged 14-3-3 protein was purified using an ÄKTA Prime (GE Healthcare, Freiburg, Germany) and Ni–NTA resin (GE Healthcare, Freiburg, Germany) according to the manufacturer's manual. The resin was washed in buffer consisting of 50 m*M* Tris–HCl, 500 m*M* NaCl, 5% glycerol, 25 m*M* imidazole and 0.5 m*M* TCEP pH 8.0. The protein was eluted in buffer consisting of 50 m*M* HEPES, 200 m*M* NaCl, 5% glycerol, 250 m*M* imidazole, 0.5 m*M* TCEP pH 8.0. The eluted protein was concentrated to 50 mg ml^{-1}, TEV protease was added to a final concentration of 1 mg ml^{-1} and cleavage was performed for 6 h at 293 K. The protein was further concentrated to a volume of 2 ml for gel filtration, which was performed using an ÄKTA Prime and a Superdex 75 16/60 gel-filtration column (GE Healthcare, Freiburg, Germany). The buffer consisted of 25 m*M* HEPES, 100 m*M* NaCl, 10 m*M* $MgCl_2$, 1 m*M* TCEP pH 8.0. The 14-3-3σ protein without His tag was then pooled according to the elution profile and concentrated to 75 mg ml^{-1}. The protein was aliquoted, flash-frozen in liquid nitrogen and stored at 193 K. The YAP pS127 peptide (^{124}RAH-pS-SPASLQ^{133}) was obtained from Biosyntan (Berlin, Germany) and its concentration was adjusted to 10 m*M*. The resuspended peptide was aliquoted, flash-frozen in liquid nitrogen and stored at 193 K.

2.4. Crystallization

For screening, the 14-3-3σ protein was complexed with the phosphopeptide at a ratio of 1:1.5 and diluted to a concentration of 10 mg ml^{-1}. For complexation, the solution was incubated for 30 min at 277 K and was then directly used for crystallization screening. Screening for suitable crystallization conditions was performed using the Qiagen JCSG Core I–IV screens (Qiagen, Hilden, Germany) with the sitting-drop vapour-diffusion method at 277 K. For the screens, Corning 3550 96-well plates (Corning, Amsterdam, Netherlands) were used; sitting drops were made by mixing 100 nl protein solution and 100 nl reservoir solution and were equilibrated against 70 µl reservoir solution. A suitable condition was optimized in a Linbro cell-culture plate (MP Biomedicals Inc., Solon, Ohio, USA) using the hanging-drop method by mixing 1 µl protein solution and 1 µl reservoir solution and equilibrating against 1 ml reservoir solution consisting of 0.095 *M* Na HEPES pH 7.4, 25.6% PEG 400, 0.19 *M* $CaCl_2$ and 5% glycerol. The obtained crystals grew within a week to dimensions of ∼400 × 100 × 100 µm and could be directly flash-cooled in mother liquor using liquid nitrogen.

2.5. Data collection, processing, structure determination and refinement

X-ray diffraction data were collected at a single wavelength of 0.855 Å on beamline X10SA at the Swiss Light Source, Paul Scherrer Institut, Villigen, Switzerland using a CCD detector. For the high-resolution setting the crystal-to-detector distance was set to 110 mm and 210 images were obtained with an oscillation of 0.5° per image. The low-resolution setting had a crystal-to-detector distance of 350 mm and 90 images were obtained with an oscillation of 1.5° per image. X-ray diffraction data were processed and scaled using *XDS* (Kabsch, 2010). Molecular replacement was carried out with the program *Phaser* (McCoy *et al.*, 2007) as part of the *CCP*4 package (Collaborative Computational Project, Number 4, 1994), using the apo structure of 14-3-3σ (PDB code 2o02) as the search model. The obtained model was subjected to iterative rounds of model building and refinement using *Coot* (Emsley & Cowtan, 2004) and *REFMAC* (Murshudov *et al.*, 1997). Figures were created using *PyMOL* (http://www.pymol.org).

3. Results

3.1. Expression, crystallization and data collection

The 14-3-3σ protein was expressed very well in *E. coli* Rosetta (DE3) cells. After purification including TEV digestion and gel filtration, a total amount of ∼25 mg protein could be obtained from 1 l culture with a purity close to 99%. On a 12% Tris–tricine gel the proteins appeared at a size that corresponded well to the 26.1 kDa calculated size of the TEV-cleaved 14-3-3σ protein.

Crystals grew within a week to dimensions of ∼400 × 100 × 100 µm in a buffer consisting of 0.095 *M* Na HEPES pH 7.4, 25.6% PEG 400, 0.19 *M* $CaCl_2$ and 5% glycerol at 277 K. The synchroton

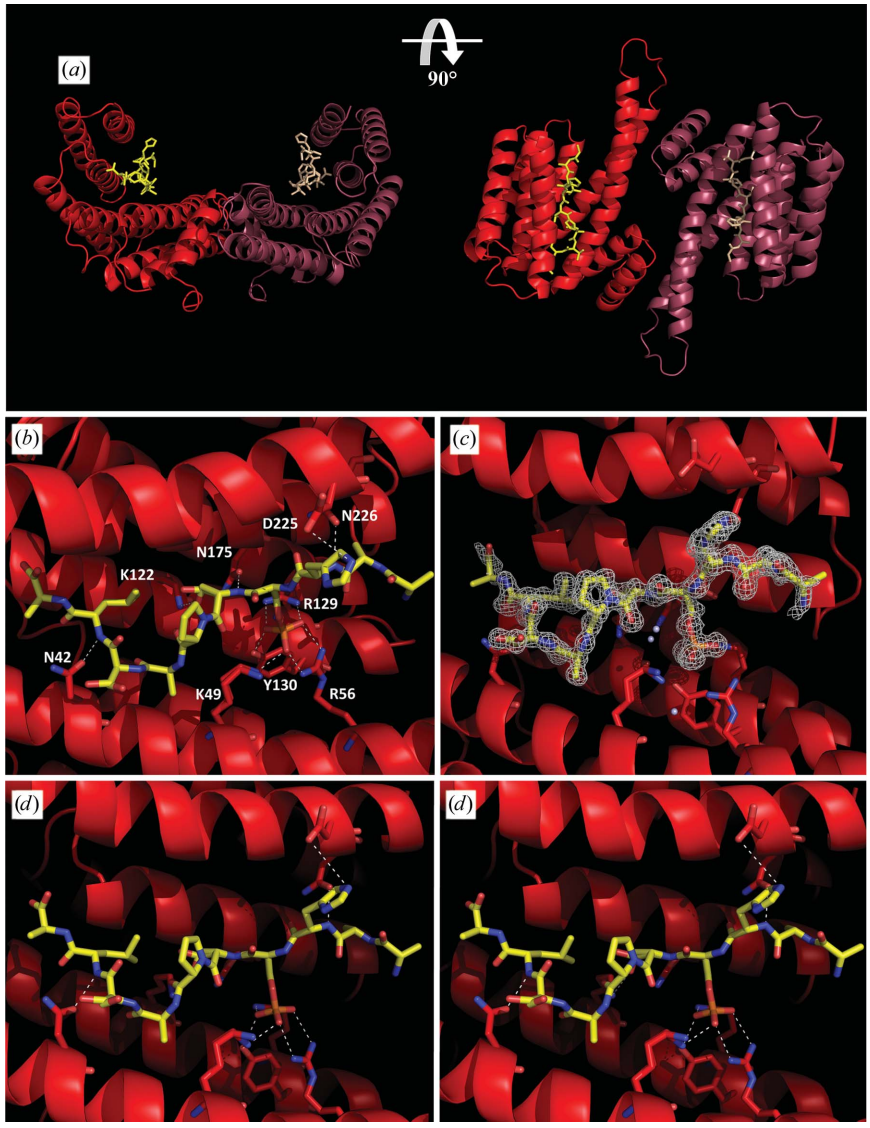

Figure 1
Structure of the 14-3-3σ–YAP pS127 peptide complex. (*a*) Cartoon representation of the 14-3-3σ dimer (red and dark red) in complex with the YAP pS127 peptide (yellow and light yellow; stick representation). The binding pocket created by helices 3, 5, 7 and 9 and the dimerization site are clearly visible, as well as the orientation of the peptide in the binding pocket. (*b*) Electrostatic interactions (dotted lines) of the phosphorylated residue pSer127 of the YAP pS127 peptide (yellow; stick representation) in the binding groove and residues Lys49, Arg56, Arg129 and Tyr130 of the 14-3-3 protein (red; cartoon representation). The backbone of the peptide is further coordinated by residues Asn42, Lys122, Asn175, Asp225 and Asn226 of the 14-3-3 protein. (*c*) A $2F_o - F_c$ electron-density map for the YAP pS127 peptide (yellow, stick representation) is shown in white. Water molecules are indicated as light blue balls. The density map is contoured at 1σ. (*d*) Stereo image of the binding pocket. Colouring is as in (*b*).

data were collected using two settings to obtain high-resolution and low-resolution diffraction data. Data were collected to 1.15 Å resolution. The crystal belonged to space group No. 20 ($C222_1$), with unit-cell parameters a = 82.27, b = 112.11, c = 62.85 Å. The Matthews coefficient suggested the presence of one 14-3-3 monomer in the asymmetric unit (V_M = 2.73 Å^3 Da^{-1}; solvent content 54.9%). For molecular replacement, *Phaser* (McCoy *et al.*, 2007) was used with the apo structure of 14-3-3σ (PDB code 2o02) as a search model and one monomer per asymmetric unit. The initial R factor for molecular replacement was 30.16% (starting value 30.29%) with a log-likelihood gain of 4554.9121 (starting value 4550.1600) as given by *Phaser*. There was a single-solution PDB-output file. The structure could be modelled using *Coot* (Emsley & Cowtan, 2004). Structure validation was performed using *REFMAC* (Murshudov *et al.*, 1997) with all H atoms included in the refinement. After iterative rounds of structure building and validation, the final model was obtained (PDB entry 3mhr; Table 1).

3.2. The YAP binding mode and comparison to known binding modes

As expected from previously solved 14-3-3 crystal structures, the 14-3-3 protein crystallizes as a dimer with the typical W-shape-like orientation of the nine α-helices in each monomer (Fig. 1*a*). The amphipathic binding groove is created by helices 3, 5, 7 and 9, while helices 1–4 participate in the dimerization of the two 14-3-3 monomers. Furthermore, the model of the 14-3-3σ–YAP pS127 peptide binary complex represents a 1:1 binding stoichiometry with respect to the 14-3-3 monomer and the peptide (Fig. 1*a*). The phosphorylated residue pSer127 of the peptide is coordinated by Lys49, Arg56, Arg129 and Tyr130 of the 14-3-3σ protein (Figs. 1*b* and 1*c*). This binding reflects the known binding mechanism of a target protein to a 14-3-3 protein. The backbone of the peptide is further coordinated by Asn42, Lys122, Asn175, Asp225 and Asn226. To date, three different

Table 1
Data and refinement statistics for the 14-3-3σ–YAP pS127 peptide complex (PDB code 3mhr).

Values in parentheses are for the highest resolution shell.

Crystal data	
Space group	$C222_1$
No. of molecules in unit cell (Z)	8
Unit-cell parameters (Å)	a = 82.27, b = 112.11, c = 62.85
Data-processing statistics	
Resolution (Å)	45.6–1.15 (1.20–1.15)
No. of unique reflections	102833 (12258)
Redundancy	5.31 (4.95)
$I/\sigma(I)$	16.54 (5.23)
Completeness (%)	99.8 (99.9)
R_{merge}	0.080 (0.351)
Structure-refinement statistics	
Resolution (Å)	45.6–1.15 (1.18–1.15)
No. of reflections	97691 (7175)
R_{work}/R_{free}	0.127/0.153 (0.129/0.170)
Reflections in test set	5142
Atomic displacement model	Anisotropic
Model statistics	
Non-H atoms	
Protein atoms	2478
Water atoms	290
Geometry: r.m.s. deviation from ideal values (count; r.m.s.; weight)	
Bonds (Å)	2246; 0.022; 0.022
Angles (°)	2084; 2.055; 1.999
Planes (Å)	2557; 0.011; 0.020
Chiral centres (Å)	343; 0.117; 0.200
Average isotropic B factor (Å^2)	
Overall	10.72
Ramachandran plot	
Most favoured region	232 [98.3%]
Allowed region	4 [1.7%]
Generously allowed and disallowed regions	0 [0.0%]

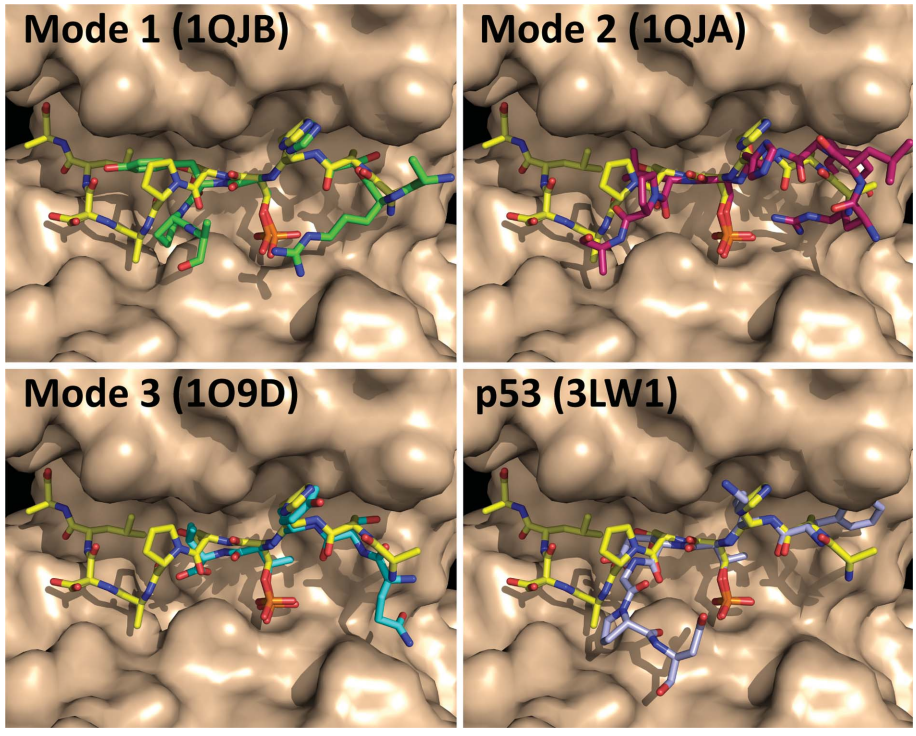

Figure 2
Comparison of the three known 14-3-3 binding motifs and the p53 pT387 peptide. The information was obtained by superimposing the YAP pS127 peptide (yellow; stick model) with PDB entries 1qjb (Rittinger *et al.*, 1999), 1qja (Rittinger *et al.*, 1999), 1o9d (Würtele *et al.*, 2003) and 3lw1 (Schumacher *et al.*, 2010). The peptides are shown as stick models (mode I in green, mode II in magenta, mode III in cyan and p53 in light blue). The 14-3-3 protein is shown as a surface representation in wheat.

binding motifs are known for 14-3-3 target proteins. In the mode III binding motif the peptide chain ends one amino acid after the phosphorylated residue and leaves the binding groove with a large open pocket, which is known to provide space for stabilizers of 14-3-3 target-protein interaction (Ottmann, Marco *et al.*, 2007; Ottmann *et al.*, 2009). As Ser127 of YAP is not positioned at the C-terminus of the full-length protein, the mode III binding motif is not represented in this case. The differences between the mode I and mode II binding motifs for this binary complex are more difficult to distinguish. Owing to the presence of a proline at the +2 position with respect to the phosphorylated residue, the peptide chain makes a kink which leads the peptide chain out of the binding pocket; the peptide exits the channel and crosses the 14-3-3 monomer in the direction of the adjacent monomer (Fig. 2). As insufficient structural information is available for full-length or larger fragments of target proteins, it remains an open question whether and how the peptide chain exits the area between the two 14-3-3 monomers. A recently published structure by our group of the p53 pT387 peptide (Schumacher *et al.*, 2010) shows a comparable trend to the mode I and II peptides, but the p53 full-length protein ends six amino acids after pThr387 and provides no further explanation regarding the orientation of the mode I or II binding motifs. Although the YAP peptide used (^{124}RAH-pS-SPASLQ^{133}) contains a proline at the +2 position, which would suggest that the peptide chain exits the binding groove, the peptide chain returns into the pocket at the position of Ser131 (Fig. 1*b*). On comparison with the structures of the mode I and II binding motifs (PDB codes 1qjb and 1qja, respectively; Rittinger *et al.*, 1999) the mode II binding motif would seem to be of more

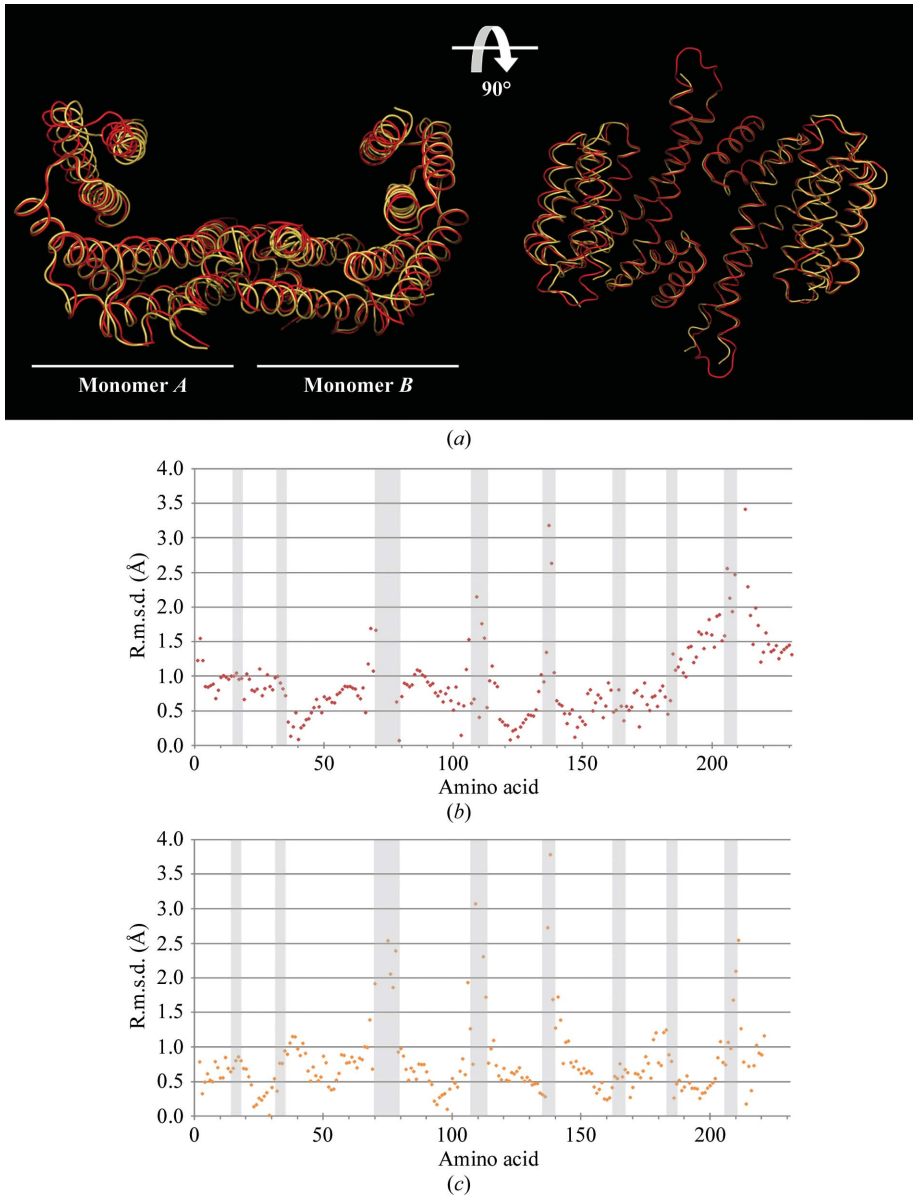

Figure 3
Comparison of 14-3-3σ apo and binary complex structures. PDB entry 1yz5 (Benzinger *et al.*, 2005) was used in an overlay with the 14-3-3σ–YAP pS127 peptide structure to determine differences in the 14-3-3 dimer. For easier comparison, the YAP pS127 phosphopeptide was removed from the structure. The overall r.m.s.d. value is 1.00321 Å. (*a*) Overlay of the two 14-3-3σ dimers shown as a cartoon representation with all helices set as loops for easier comparison. The 14-3-3σ of PDB entry 1yz5 is shown in yellow, while the 14-3-3σ of the YAP pS127 peptide complex is shown in red. (*b*) R.m.s.d. values (Å) for the comparison of monomer *A* in the two 14-3-3σ structures. The loop regions are indicated by grey rectangles. The graph shows the differences in Å for corresponding C^{α} atoms in the 14-3-3σ backbone. (*c*) R.m.s.d. values (Å) for the comparison of monomer *B* in the two 14-3-3σ structures. The loop regions are indicated by grey rectangles.

interest in this context, because in the case of 1qja the peptide chain also seems to make a second kink and point back in the direction of the binding pocket. Therefore, the YAP pS127 peptide shows a comparable mode II binding motif (Fig. 2).

3.3. Comparison of the 14-3-3σ apo structure and the 14-3-3σ–YAP pS127 peptide structure

In 2005, Benzinger and coworkers solved the crystal structure of the 14-3-3σ apoprotein to 2.8 Å resolution (PDB entry 1yz5; Benzinger *et al.*, 2005). To determine whether the binding of a phosphopeptide leads to a different orientation of the α-helices in the 14-3-3 protein, an overlay was performed in order to analyse the root-mean-square deviation (r.m.s.d.) value for the two crystal structures (Fig. 3*a*). The calculated overall r.m.s.d. of the two structures was 1.00321 Å. Further comparison revealed that the dimerization interface, which is represented by helices 1–4, has very low r.m.s.d. values for individual amino acids (Figs. 3*b* and 3*c*). Apart from the regions of the loops, the r.m.s.d. is around 1 Å or lower. Interestingly, in monomer *A* the r.m.s.d. value for helices 8 and 9 increases dramatically compared with the remaining amino acids of the structure (Fig. 3*b*). It is of interest that the red-coloured 14-3-3 ribbon structure points in the direction of the binding groove and that this red structure represents the 14-3-3–YAP pS127 complex structure.

4. Discussion

The model shows how one YAP pS127 peptide is bound to one 14-3-3 monomer (Fig. 1*a*). The binding of the peptide is in alignment with previously observed bound peptides. The phosphate at Ser127 of the peptide is coordinated by Lys49, Arg56, Arg129 and Tyr130 of the 14-3-3σ protein (Figs. 1*b* and 1*c*). Compared with the other three binding motifs, the orientation of the peptide in the cavity is comparable to motif II with respect to the structure. From a sequence point of view, the N-terminus of the peptide fits more closely to a mode I binding motif. However, as the sequence following the phosphorylated residue seems to play a more important role in the binding and coordination of the binding motif in the cavity, we suggest that the structure of the YAP pS127 peptide in complex with 14-3-3σ adds another putative mode II structure to the collection of 14-3-3 structures. In addition to this, the advantage of this structure is that the peptide chain is longer as in 1qja (Rittinger *et al.*, 1999) and it can be seen that a putative mode II binding motif can kink back into the binding groove and point towards the open end of the pocket, thereby completing the picture of how mode II binding partners of 14-3-3 proteins might be coordinated in the binding cavity.

Comparison of the structure presented here and the 14-3-3σ apo structure (PDB entry 1yz5; Benzinger *et al.*, 2005) showed a slight movement of helices 8 and 9 in the binary complex structure with the 14-3-3–YAP pS127 peptide (Fig. 3). Although speculative, it might be possible that the shift in the orientation of these helices compared with the apo structure indicates a tightening of the binding groove upon binding of a peptide. Furthermore, it is of interest that the remaining helices, especially those in the dimerization interface, seem to be more tightly fixed in the dimer. This indicates that a possible movement of the 14-3-3 protein helices is concentrated on the outermost helices 8 and 9 and that this increases the binding interface of the target protein and the 14-3-3 protein.

As shown by our recent publication (Schumacher *et al.*, 2010), this crystallization condition can be used to solve the structures of complexes of different kinds of phosphopeptides with 14-3-3σ. Although 14-3-3σ is not the natural 14-3-3 binding background for all reported interactions, the 14-3-3σ isoform crystallizes as crystals that diffract to high resolution largely independently of the bound peptide. Therefore, this condition might be used as a tool to investigate the orientation and structural binding mechanistics for peptides of 14-3-3 target proteins up to a length of 14 amino acids (unpublished data). Additionally to the binding characteristics, these high-resolution structures provide a tool for *in silico* ligand docking for drug development. With respect to drug development, high-resolution structures have the advantage of providing more detailed information for docking programs. In the case that a suitable compound is found in the docking, the presented method is also suitable for the soaking and cocrystallization of small molecules (manuscript in preparation). Additionally, as the crystallization of longer fragments or even full-length target proteins is presently the limiting step, it is necessary to find a tool to investigate the different binding mechanisms of the different target proteins. Although the peptides might be orientated differently in longer fragments or in the context of the full-length protein, the peptide would provide an initial starting point for mutagenesis analysis or other ways of investigating and manipulating the binding mechanisms.

We thank the staff at beamline X10SA of the Swiss Light Source for support during crystallographic data collection, and we are thankful to Dr Thomas Barends and Dr Anton Meinhart for collecting the data at the SLS.

References

Benzinger, A., Popowicz, G. M., Joy, J. K., Majumdar, S., Holak, T. A. & Hermeking, H. (2005). *Cell Res.* **15**, 219–227.
Collaborative Computational Project, Number 4 (1994). *Acta Cryst.* D**50**, 760–763.
Emsley, P. & Cowtan, K. (2004). *Acta Cryst.* D**60**, 2126–2132.
Ferl, R. J., Manak, M. S. & Reyes, M. F. (2002). *Genome Biol.* **3**, reviews3010.
Hao, Y., Chun, A., Cheung, K., Rashidi, B. & Yang, X. (2008). *J. Biol. Chem.* **283**, 5496–5509.
Hermeking, H. (2003). *Nature Rev. Cancer*, **3**, 931–943.
Hermeking, H. & Benzinger, A. (2006). *Semin. Cancer Biol.* **16**, 183–192.
Kabsch, W. (2010). *Acta Cryst.* D**66**, 125–132.
Kostelecky, B., Saurin, A. T., Purkiss, A., Parker, P. J. & McDonald, N. Q. (2009). *EMBO Rep.* **10**, 983–989.
Lei, Q.-Y., Zhang, H., Zhao, B., Zha, Z.-Y., Bai, F., Pei, X.-H., Zhao, S., Xiong, Y. & Guan, K.-L. (2008). *Mol. Cell. Biol.* **28**, 2426–2436.
Macdonald, N., Welburn, J. M., Nguyen, A., Yaffe, M. B., Clynes, D., Moggs, J. G., Orphanides, G., Thomson, S., Edmunds, J. W., Clayton, A. L., Endicott, J. A. & Mahadevan, L. C. (2005). *Mol. Cell*, **20**, 199–211.
McCoy, A. J., Grosse-Kunstleve, R. W., Adams, P. D., Winn, M. D., Storoni, L. C. & Read, R. J. (2007). *J. Appl. Cryst.* **40**, 658–674.
Mhawech, P. (2005). *Cell Res.* **15**, 228–236.
Murshudov, G. N., Vagin, A. A. & Dodson, E. J. (1997). *Acta Cryst.* D**53**, 240–255.
Muslin, A. J., Tanner, J. W., Allen, P. M. & Shaw, A. S. (1996). *Cell*, **84**, 889–897.
Obsil, T., Ghirlando, R., Klein, D. C., Ganguly, S. & Dyda, F. (2001). *Cell*, **105**, 257–267.
Oka, T., Mazack, V. & Sudol, M. (2008). *J. Biol. Chem.* **283**, 27534–27546.
Ottmann, C., Marco, S., Jaspert, N., Marcon, C., Schauer, N., Weyand, M., Vandermeeren, C., Duby, G., Boutry, M., Wittinghofer, A., Rigaud, J. & Oecking, C. (2007). *Mol. Cell*, **25**, 427–440.
Ottmann, C., Weyand, M., Sassa, T., Inoue, T., Kato, N., Wittinghofer, A. & Oecking, C. (2009). *J. Mol. Biol.* **386**, 913–919.
Ottmann, C., Yasmin, L., Weyand, M., Veesenmeyer, J. L., Diaz, M. H., Palmer, R. H., Francis, M. S., Hauser, A. R., Wittinghofer, A. & Hallberg, B. (2007). *EMBO J.* **26**, 902–913.
Rittinger, K., Budman, J., Xu, J., Volinia, S., Cantley, L. C., Smerdon, S. J., Gamblin, S. J. & Yaffe, M. B. (1999). *Mol. Cell*, **4**, 153–166.
Schumacher, B., Mondry, J., Thiel, P., Weyand, M. & Ottmann, C. (2010). *FEBS Lett.* **584**, 1443–1448.

Tzivion, G., Gupta, V. S., Kaplun, L. & Balan, V. (2006). *Semin. Cancer Biol.* **16**, 203–213.
Wang, K., Degerny, C., Xu, M. & Yang, X.-J. (2009). *Biochem. Cell Biol.* **87**, 77–91.
Würtele, M., Jelich-Ottmann, C., Wittinghofer, A. & Oecking, C. (2003). *EMBO J.* **22**, 987–994.
Yaffe, M. B., Rittinger, K., Volinia, S., Carson, P. R., Aitken, A., Leffers, H., Gamblin, S. J., Smerdon, S. J. & Cantley, L. C. (1997). *Cell*, **91**, 961–971.
Zhang, L., Ren, F., Zhang, Q., Chen, Y., Wang, B. & Jiang, J. (2008). *Dev. Cell*, **14**, 377–387.
Zhao, B. *et al.* (2007). *Genes Dev.* **21**, 2747–2761.